International Journal of Heat and Mass Transfer 131 (2019) 167–175

Contents lists available at ScienceDirect

International Journal of Heat and Mass Transfer

journal homepage: www.elsevier.com/locate/ijhmt

Full-spectrum correlated-*k*-distribution look-up table for use with radiative Monte Carlo solvers

Chaojun Wang [a], Michael F. Modest [b,*], Boshu He [a,c]

[a] Institute of Combustion and Thermal Systems, School of Mechanical, Electronic and Control Engineering, Beijing Jiaotong University, Beijing 100044, People's Republic of China
[b] School of Engineering, University of California, Merced 95340, USA
[c] School of Mechanical and Power Engineering, Haibin College of Beijing Jiaotong University, Huanghua 061199, Hebei Province, People's Republic of China

ARTICLE INFO

Article history:
Received 12 June 2018
Received in revised form 26 October 2018
Accepted 29 October 2018
Available online 17 November 2018

Keywords:
Radiative heat transfer
Full-spectrum correlated-*k*-distribution (FSCK)
Photon Monte Carlo (PMC)
Look-up table
Random-number database
Nonhomogeneous media

ABSTRACT

The full-spectrum correlated-*k*-distribution (FSCK) look-up table previously developed by the authors Wang et al. (2018) provides an efficient means for accurate calculations of radiative properties in nonhomogeneous media in conjunction with conventional radiative transfer equation (RTE) solvers. However, the current FSCK look-up table cannot be combined with statistical RTE solvers. A random-number relation was derived using the new implementation proposed in Wang et al. (2018) for the use of FSCK tables together with photon Monte Carlo (PMC) RTE solvers, and a corresponding random-number database including CO_2, H_2O, CO and soot has been constructed. Radiative heat transfer for two realistic scaled flames is studied to test the performance of the FSCK/PMC method using both FSCK look-up table and random-number database. Results show that the FSCK/PMC method can achieve almost the same accuracy but at cheaper computational cost and much lower memory requirement compared to the benchmark line-by-line solutions.

1. Introduction

Due to their dramatic variation across the spectrum, radiative properties, especially those of gases and soot in high-temperature environments, display very strong spectral, or 'non-gray' behavior, which is both very difficult to characterize and to evaluate [1]. Line-by-line (LBL) calculations can resolve all of the spectral variations and therefore provide the most accurate radiative properties [2]. However, LBL modelling requires absorption coefficients for over one million wavenumbers and radiative transfer equation (RTE) evaluations of the same number, making it prohibitive in practical simulations because of the computational power needed. This has led to gradual development of accurate and efficient spectral models, among which the full-spectrum *k*-distribution (FSK) method developed by Modest [3] has become one of the most promising methods. Based on the reordering concept, the FSK method collects spectral absorption coefficients into *k*-distributions, with a single *k*-value corresponding to the same absorption coefficient at many wavenumbers. With spectral integration performed by using high-accuracy Gauss quadrature, the FSK method can reduce the number of RTE evaluations from over one million to around ten without losing accuracy.

To avoid the cumbersome processes of both assembling and mixing *k*-distributions, Wang et al. [4–6] constructed an FSK look-up table for mixtures of CO_2, H_2O, CO and soot, in which standard *k*-distributions were stored. The required correlated *k*-values used during the radiative calculations can be obtained by several interpolations among those standard *k*-distributions. Recently, by applying the correlation principle an additional time, they developed an upgraded full-spectrum correlated-*k*-distribution (FSCK) look-up table [7]. In the latest database the correlated *k*-values corresponding to fixed quadrature values (g) are directly tabulated for each thermodynamic state. During radiative calculations, the correlated *k*-values can be readily obtained from the tabulated values without additional interpolations and, therefore, the efficiency using the FSCK look-up table was further improved.

The FSCK look-up table has been proven to be able to achieve near LBL accuracy in nonhomogeneous media with only a tiny fraction of the LBL computational cost [7]. However, it has a limitation that the current table can be only combined with conventional RTE solvers, such as the spherical harmonics (P_N) solver [8,9] and the discrete ordinates (S_N) solver [10,11]. Unlike conventional RTE solvers, statistical RTE solvers are based on ray tracing, among which the photon Monte Carlo (PMC) solver is the most promising one. Since energy travels in discrete photons over relatively long distances along a straight path before interaction with matter, the PMC solver is particularly well suited for radiative transfer

* Corresponding author.
E-mail address: mmodest@ucmerced.edu (M.F. Modest).

https://doi.org/10.1016/j.ijheatmasstransfer.2018.10.133
0017-9310/

Nomenclature

a	nongray stretching function in FSK method, –
$\bar{a}$	weight function in SLW method
E	total energy, W/m^3
F_s	absorption distribution function
f	full-spectrum k-distribution, m
f_v	soot volume fraction, –
g	cumulative full-spectrum k-distribution, -
I	radiative intensity, W/(m^2·sr)
k	absorption coefficient variable, m^{-1}
M	number of subsamples, –
N	number of rays, –
p	total pressure, bar
q	radiative heat flux, W/m^2
T	temperature, K
R	random number, –
$S(\cdot)$	subsample, –
s	path length, m
$\hat{\mathbf{s}}$	direction vector, –
r	radius length, m
V	cell volume, m^3
x	mole fraction, –
z	axial length, m

Greek symbols

$\delta(\cdot)$	dirac-delta function, –
ϕ	vector of local thermodynamic state variables, –
η	wavenumber, m^{-1}
κ_η	spectral absorption coefficient, m^{-1}
κ_P	Planck-mean absorption coefficient, m^{-1}
σ	Stephan-Boltzmann constant, 5.67×10^{-8} W/(m^2·K^4)
σ_m	standard deviation, –
σ_s	scattering coefficient, m^{-1}
Φ	scattering phase function, –
Ω	solid angle, sr

Subscripts

abs	absorption
b	blackbody
p	pressure-based

Superscripts

0	reference state

Abbreviations

ADF	absorption distribution function
FSK	full-spectrum k-distribution
FSCK	full-spectrum correlated-k-distribution
LBL	line-by-line
PMC	photon Monte Carlo
RTE	radiative transfer equation
SLW	spectral-line-based weighted-sum-of-gray-gases
TRI	turbulence-radiation interaction

problems by tracing the history of a statistically meaningful random sample of photons from their points of emission to their points of absorption [12]. With sufficient photons, the PMC solver can statistically provide the exact solution, making it the benchmark solver in high-dimensional geometries. In essence, the PMC solver does not need to solve the RTE and, therefore, can be applied to problems of arbitrary difficulty with relative ease. Its stochastic nature also makes it the only solver capable of fully evaluating scattering or turbulence-radiation interactions (TRI). A well-known disadvantage of this solver is its high computational cost for the large amount of ray tracing required. However, this becomes ever less important with the rapid increase of computational capacity and the development of parallel computing, which makes the PMC solver most promising among the various solution methods for the RTE. In addition, PMC calculations are often used to test the accuracy of conventional models.

The first application of the PMC method in radiative heat transfer was for a gray gas [13]; only in the 1990s was it demonstrated by Modest [14] how nongray gas properties can be considered (using the statistical narrow-band model), which was later also employed by Cherkaoui et al. [15]. Farmer and Howell showed the exponential wide-band model can also be incorporated into the PMC simulation [16,17]. Of course, these implementations suffer the same inaccuracies as their underlying spectral models. More recently, Wang et al. [18] implemented the most accurate LBL method into a PMC solver (LBL/PMC) in the field of combustion, and Ozawa et al. [19] and Feldick et al. [20] applied it to hypersonic plasmas. In their work, a random-number relation was developed to choose the wavenumbers with substantial emission and thus fewer wavenumbers were required to yield accuracy comparable to the one obtained from standard spectral integration. Furthermore, Ren et al. [21] developed a hybrid wavenumber selection scheme for the LBL/PMC method in high-temperature gaseous media, achieving a significant improvement in efficiency.

While the near LBL accuracy can be achieved, the current FSCK tables cannot be directly combined with the PMC solver due to the lack of a random-number database for artificial wavenumber selection. Hence, combining the FSCK look-up table with the PMC solver becomes desirable and attractive. Wang et al. [22] designed a preliminary FSCK/PMC solver for nonhomogeneous media with random-number databases constructed on-the-fly. Because of the tedious construction process, the computational cost using this FSCK/PMC method was considerably larger than that using the benchmark LBL/PMC method. The goal of the present work is to construct a random-number database for the latest FSCK look-up table so that the FSCK/PMC method can be accurately and efficiently used for radiative calculations. Here, a random-number relation has been derived using the new implementation proposed in [7], and details of the construction will be presented. Radiative heat transfer for two realistic scaled flames is studied to verify the accuracy and efficiency of the FSCK/PMC method. Results show that using the random-number database developed in this work together with the FSCK look-up table can provide similar accuracy but at somewhat cheaper computational cost and extremely lower memory requirement compared to benchmark LBL/PMC solutions.

2. Theoretical background

2.1. Full-spectrum correlated-k-distribution method

A full-spectrum k-distribution is a reordered absorption coefficient that accounts for the variation of the Planck function and is defined as [12]

$$f_{T_P,\phi}(k) = \frac{1}{I_b(T_P)} \int_0^\infty I_{b\eta}(T_P)\delta(k - \kappa_\eta(\boldsymbol{\phi}))\mathrm{d}\eta \tag{1}$$

where κ_η is the spectral absorption coefficient calculated from a spectroscopic database; $\delta(\cdot)$ is the Dirac-Delta function; $\boldsymbol{\phi}$ is a vector of local thermodynamic state variables including pressure, temperature and species concentration; $f_{T_P,\phi}(k)$ is a Planck-function-weighted k-distribution with absorption coefficient evaluated at the local state $\boldsymbol{\phi}$ and a Planck function temperature T_P; I_b and $I_{b\eta}$ are the Planck function and the spectral Planck function, respectively; η is the wavenumber.

The cumulative full-spectrum k-distribution is defined as

$$g_{T_P,\phi}(k) = \int_0^k f_{T_P,\phi}(k')\mathrm{d}k' \tag{2}$$

Thus, g represents the fraction of the spectrum whose absorption coefficient lies below the value of k and, therefore, $0 \le g \le 1$. Inverting Eq. (2), a smooth, monotonically increasing function, $k_{T_P,\phi}(g)$, can be obtained, with minimum and maximum values identical to those of the absorption coefficients.

To apply the FSK method for a nonhomogeneous mixture, radiative properties need to be transformed into a unified reference g-space (g^0), which is usually achieved by employing the correlation principle as follows

$$g_{T_P,\phi^0}(k) = g_{T_P,\phi}(k^*) \tag{3}$$

and the FSK based on Eq. (3) is the so-called full-spectrum correlated-k-distribution (FSCK) method. Note that the FSCK method is approximate since the correlation principle can never be truly achieved in nonhomogeneous media. The radiative transfer equation (RTE) in FSCK form can be expressed as

$$\frac{\mathrm{d}I_g}{\mathrm{d}s} = k^*(g^0)\left[a(g^0)I_b(T_P) - I_g\right] - \sigma_s\left(I_g - \frac{1}{4\pi}\int_{4\pi} I_g(\hat{\mathbf{s}}')\Phi(\boldsymbol{\phi},\hat{\mathbf{s}},\hat{\mathbf{s}}')\mathrm{d}\Omega'\right) \tag{4}$$

where it is assumed that the scattering properties, σ_s and Φ, are gray, and,

$$I_g = \int_0^\infty I_\eta \delta(k - \kappa_\eta(\boldsymbol{\phi}^0))\mathrm{d}\eta / f_{T^0,\phi^0}(k) \tag{5}$$

$$a(g^0) = \frac{f_{T_P,\phi^0}(k)}{f_{T^0,\phi^0}(k)} = \frac{\mathrm{d}g_{T_P,\phi^0}(k)}{\mathrm{d}g^0_{T^0,\phi^0}(k)} \tag{6}$$

$k^*(g^0)$in Eq. (4) represents a correlated k-value in reference g-space.

In addition, if Eq. (4) is integrated using a trapezoidal scheme, i.e., the variable absorption coefficient $k^*(g^0)$ is replaced by a single, constant value $\tilde{k}_i(T_P,\boldsymbol{\phi})$ for the ith finite range of F_s spanning across $F_{s,i-1} < F_s \le F_{s,i}$, integration of Eq. (4) over the ith F_s-range leads to

$$\frac{\mathrm{d}I_i}{\mathrm{d}s} = \tilde{k}_i(T_P,\boldsymbol{\phi})\left[\bar{a}_i(T_P,T^0)I_b(T_P) - I_i\right] - \sigma_s\left(I_i - \frac{1}{4\pi}\int_{4\pi} I_i(\mathbf{s}')\Phi(\boldsymbol{\phi},\hat{\mathbf{s}},\hat{\mathbf{s}}')\mathrm{d}\Omega'\right), i = 1,\ldots,N \tag{7}$$

where $\bar{a}_i(T_P,T^0)$ represents the weight function and is evaluated as [1]

$$\bar{a}_i(T_P,T^0) = F_{s,i} - F_{s,i-1} \tag{8}$$

This is known as the spectral-line-based weighted-sum-of-gray-gases (SLW) method developed by Dension and Webb [23]. Generally, the values of $\tilde{k}_i(T_P,\boldsymbol{\phi})$ and $\bar{a}_i(T_P,T^0)$ are obtained from the absorption distribution function (ADF) [24–27], for which the SLW method becomes the ADF method. Comparison of Eqs. (4) and (7) shows that, mathematically, the SLW (or ADF) method is simply the FSCK method with a simple step integration scheme. Moreover, the F_s in the SLW (or ADF) method and the g in the FSCK method can be expressed using the same equation [28]. Therefore, any database or models developed for the FSCK method should be also valid for the SLW method or the similar ADF method.

2.2. Photon Monte Carlo solver

During numerical calculations, the physical domain is usually discretized into a number of finite subvolumes (cells) for simulation. Gas molecules in each cell continuously emit energy in the form of photons into random directions and these photons may be absorbed or scattered by the molecules in other cells during transmission. The PMC solver directly simulates such processes by releasing representative photon bundles (rays) carrying an amount of energy from each cell into random directions. The absorbed energy by the cell through which a specific photon ray passes can be expressed as

$$E_{\mathrm{abs}} = E(1 - e^{-\kappa s}) \tag{9}$$

where E is the energy of the ray before entering the cell and s is the path length of the ray through the cell. In nongray simulations, each photon ray is assigned a representative spectral variable depending on statistical random-number relation. This allows spectral variations to be accurately resolved with a sufficient number of rays. After all rays have been traced until they are absorbed or escape from the domain, the negative radiative heat source, $\nabla \cdot q$, for each cell, e.g., cell i, can be easily evaluated from

$$\nabla \cdot q_i = 4\kappa_{P,i}\sigma T_i^4 - \sum_{j=1}^{\mathrm{J}} E_{\mathrm{abs},j}/V_i \tag{10}$$

where κ_P is the Planck-mean absorption coefficient, σ is the Stephan-Boltzmann constant, J denotes the number of rays that passed through cell i and V_i is the cell volume. The first term on the right hand side is the total emission from cell i and the second term collects all energy absorbed by cell i, both per unit volume.

Since the PMC solver is based on statistical methods, the estimated sampling error $S(N)$ may be obtained by collecting a number of M subsamples, $S(N_m)$. Normally, each subsample would trace identical amounts of rays, leading to [12],

$$N_m = N/M; \quad m = 1,2,\ldots,M \tag{11}$$

$$S(N) = \frac{1}{M}\sum_{m=1}^{M} S(N_m) \tag{12}$$

The M subsamples may then be treated as if they were independent experimental measurements of the same quantity. Then, the variance or adjusted mean square deviation of the mean can be calculated as,

$$\sigma_m^2 = \frac{1}{M(M-1)}\sum_{m=1}^{M}[S(N_m) - S(N)]^2 \tag{13}$$

The central limit theorem states that the mean $S(N)$ of M measurements, $S(N_m)$, follows a Gaussian distribution, whatever the distribution of the individual measurements. This implies that there is 68.3% confidence that the correct answer, $S(\infty)$, lies within the limits of $S(N) \pm \sigma_m$, 95.5% confidence within $S(N) \pm 2\sigma_m$, or 99% confidence within $S(N) \pm 2.58\sigma_m$.

2.3. Implementation of FSCK method into PMC solver

The key element to incorporate the FSCK method into a PMC solver is to determine statistically meaningful spectral variables, g^0, for the photon rays to be traced for which the spectral property, k^*, can be found accordingly. Since the energy carried by each ray is part of local emission from its cell, the relation of random-number and spectral variable is always defined based on emission. In the transformed RTE shown in Eq. (4), the full integration from 0 to 1 of the first term in the bracket on the right hand side represents the local emission and, therefore, the random-number relation can be expressed as

$$R(g^0) = \frac{\int_0^{g^0} k^*(g^0)a(g^0)dg^0}{\int_0^1 k^*(g^0)a(g^0)dg^0} \tag{14}$$

where R is a random number, which represents fractional emission for the artificial wavenumber range $(0 \rightarrow g^0)$. Given an arbitrary R, the corresponding spectral variable, g^0, can be determined by inverting Eq. (14).

In order to determine the correlated k-values, $k^*(g^0)$, several implementations have been proposed and summarized in [7], including the original implementation, Cai's implementation and the latest implementation developed in [7]. Since the newest version [7] is most compact and computer time efficient, it is employed here.

At the heart of this tabulation is the idea to employ the correlation principle twice, i.e.,

$$g_{T^0,\phi(T^0,\mathbf{x}^0)} = g_{T^0,\phi(T^0,\mathbf{x})} \tag{15}$$

and

$$g_{T,\phi(T^0,\mathbf{x})} = g_{T,\phi(T,\mathbf{x})} \tag{16}$$

where for clarity, the state ϕ is written out here to show its sub-variables, i.e., temperature and species concentrations. Equation (15) implies that the reference state is treated to be a function of the reference temperature only while Eq. (16) is used for the implementation of interpolations to find correlated k-values on the local standard k-distribution, details of which can be found in [7]. With both equations, the correlated k-values and the a-values can be expressed as

$$k^*(g^0) = k_{T,\phi(T,\mathbf{x})}\left(g_{T^0,\phi(T^0,\mathbf{x})}\right) = k_{T,\phi(T,\mathbf{x})}\left(g_{T,\phi(T^0,\mathbf{x})}\right) \tag{17}$$

$$a(g^0) = a\left(g_{T^0,\phi(T^0,\mathbf{x})}\right) = \frac{\mathrm{d}g_{T,\phi(T^0,\mathbf{x})}}{\mathrm{d}g_{T^0,\phi(T^0,\mathbf{x})}} \tag{18}$$

This scheme gives a correlated k-distribution, for which the correlated k-values are in the reference g-space and, therefore, can be directly used in nonhomogeneous media. It has been verified to conserve emission, i.e.,

$$\kappa_P = \int_0^1 k^*(g^0)a(g^0)\mathrm{d}g^0 \tag{19}$$

and was found to be error-free for radiative calculations in realistic flames [7].Employing Eqs. (17)–(19), the random-number relation shown in Eq. (14) can be written as

$$R(g^0) = R\left(g_{T^0,\phi(T^0,\mathbf{x})}\right) = \frac{\int_0^{g_{T^0,\phi(T^0,\mathbf{x})}} k_{T,\phi(T,\mathbf{x})}\left(g_{T^0,\phi(T^0,\mathbf{x})}\right)a\left(g_{T^0,\phi(T^0,\mathbf{x})}\right)\mathrm{d}g_{T^0,\phi(T^0,\mathbf{x})}}{\kappa_P} \tag{20}$$

where the reference g-space has been replaced by $g_{T^0,\phi(T^0,\mathbf{x})}$ and the R-g^0 relation is determined by the triple dependency k-values, $k_{T,\phi(T,\mathbf{x})}\left(g_{T^0,\phi(T^0,\mathbf{x})}\right)$. This leads to the convenience that the random-number relation can be tabulated into a relatively small database, using which the artificial wavenumber, g^0 (or $g_{T^0,\phi(T^0,\mathbf{x})}$), can be selected. Together with the FSCK look-up table developed in [7], the FSCK method can be readily incorporated into a PMC solver.

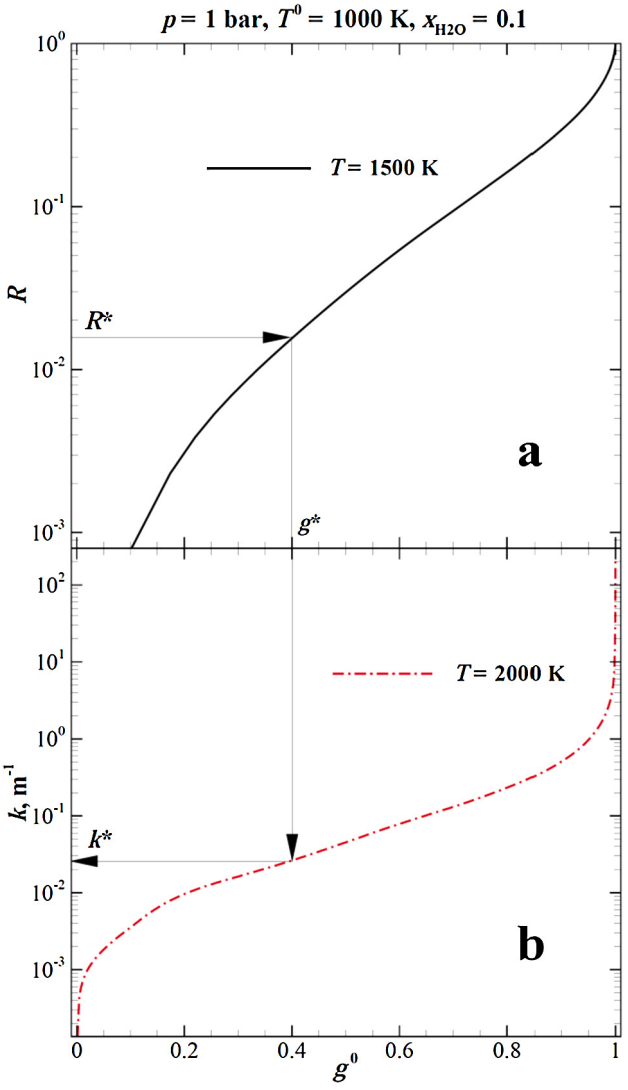

Fig. 1. Determinations of (a) artificial wavenumber from the R-g^0 relation and (b) spectral property from the correlated k-distribution during ray tracing.

The detailed selection process for a ray to be traced in a domain filled with a 10% H_2O-90% N_2 mixture is illustrated in Fig. 1, assuming that the reference temperature is 1000 K and the local temperature of the cell that emits the ray is 1500 K. Before launch, each ray needs to be assigned a statistically determined spectral location by picking a random number R^*. Then, the corresponding spectral variable, g^*, can be found from the R-g^0 relation as shown in Fig. 1a. Employing the new FSCK tabulation of [7] for the R-g^0 relation given by Eq. (20), g^* belongs to the reference g-space and can be carried by the ray until it is absorbed or escapes from the domain. When the ray travels through other cells, e.g., a cell whose local temperature is 2000 K, the energy absorbed by the cell needs to be determined with the local spectral properties. Since the implementation in [7] has transformed those local k-values into the reference g-space, the spectral property, k^*, can be readily obtained according to g^* from the correlated k-distribution as shown in Fig. 1b.

3. Construction of random-number database

To construct the random-number database, the R-g^0 relation described by Eq. (20) needs to be known for each thermodynamic state to be tabulated, leading to the requirement of k-distributions partially integrated from 0 to g^0. Note that the k-distribution in Eq. (20) represents the correlated k-distribution rather than the standard k-distribution. The detailed approach to generate those correlated k-distributions was developed in [7], and is outlined here for completeness: three standard k-distributions are first generated using the LBL database [29] for gases (updated to HITEMP2010 [30]) and the correlations [31] for soot, followed by employment of the new scheme to obtain the correlated k-distributions. In order to guarantee the accuracy of partial integration from 0 to g^0 of Eq. (20), 5000 correlated k-values are chosen to represent a single correlated k-distribution at each thermodynamic state, resulting in 5000 values for each raw R-g^0 relation. Since g^0 is to be found from a picked random number set, to avoid unnecessary iterations, these values are recast into a g^0-R table.

In practical applications, the raw g^0-R relation with 5000 values at each thermodynamic state is unacceptable due to the large storage requirement. Since the random number R always varies between 0 and 1, fixing R-values is a logical choice to reduce storage, and 32 Gauss-Chebyshev quadrature points were chosen as fixed R-values to store g^0-values for the random-number database developed in this work. The sufficiency of the selected number of R-values for each state is well demonstrated by the example shown in Fig. 2, in which emission and negative radiative heat source $\nabla \cdot q$ of a nonhomogeneous 25% H_2O-75% N_2 mixture across a 1D slab bounded by two cold black walls are evaluated with both the LBL method and the FSCK method combined with the PMC solver. The LBL calculations provide a reference solution, employing the random-number database for the LBL/PMC method as developed in [21]. For the FSCK/PMC method, the g^0-values are obtained from the raw g^0-R relation by using three different databases, using 8, 16 and 32 R-values for each state, respectively, with R-values taken from the respective Chebyshef quadrature sets. Similarly, the needed k-values for absorption are found from the correlated k-distributions with the same number of 8, 16 and 32 g^0-values. In all PMC calculations, 10 runs/trials are carried out with 100,000 photon rays used for each test to make the standard deviations as low as possible. In Fig. 2, the standard deviations for $\nabla \cdot q$ are shown as error bars and are very small, demonstrating the high confidence of the calculations. It can be seen that using a small number of data points for $g^0(R)$ and $k(g^0)$, e.g., 8, can give good predictions of emission but large discrepancies of $\nabla \cdot q$ are found compared to benchmark LBL/PMC results. The reason is that accurate emission values are built into the PMC scheme, while interpolation errors in $g^0(R)$ lead to statistically inaccurate spectral g^0-values and, more importantly, interpolation errors in $k(g^0)$ lead to inaccurate absorption values. When the number of data points for $g^0(R)$ and $k(g^0)$ are equal to or larger than 16, the results tend to be error-free. Therefore, at least 16 points for each state should be employed for the FSCK/PMC method. To further guarantee accuracy for any optical conditions, 32 R-values for each state were used to store corresponding g^0-values for the random-number database developed in this work, and the correlated k-distributions in Eq. (17) required for absorption should also be used with 32 data points.

Because of both mixing and self-broadening, the correlated k-distributions may show nonlinearities [4–7]. This inevitably results in nonlinearities of g^0-R relations since they are calculated from correlated k-distributions. As shown in Fig. 3, the exact g^0-values corresponding to different tabulated R-values may deviate from the respective linear dash-dot lines with increasing mole fraction of CO_2. To mitigate those nonlinear effects, the number of data-based gas mole fractions or soot volume fractions where conspicuous variations occur were increased, which also applies for the FSCK look-up tables. Different from the correlated k-distributions that are always monotonically increasing with gas mole fraction or soot volume fraction [7], the g^0-values are non-monotonic and range between 0 and 1, which may give different nonlinear behavior. For example, the nonlinearities of g^0-values shown in Fig. 3 are stronger than those of corresponding correlated k-values, and different nonlinearities can be found for different fixed R-values even at the same thermodynamic state. Note that the variations of g^0-values may be relatively small, e.g., less than 0.0005 in Fig. 3; however, it is found that radiative calculations are very sensitive to those small variations. Furthermore, it was observed that most nonlinearities for gas mixtures occur at low mole fractions, leading to the need of including several low mole fraction data points in the database. For soot the nonlinear behavior is found to be strong at small fixed R-values, where shows

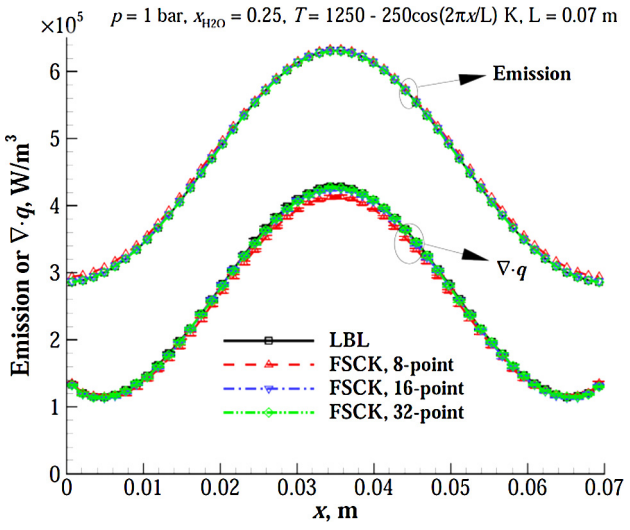

Fig. 2. Comparison of emission and negative radiative heat source across a 1D slab using LBL and FSCK methods combined with a PMC solver; three sets of quadrature are used for the FSCK method.

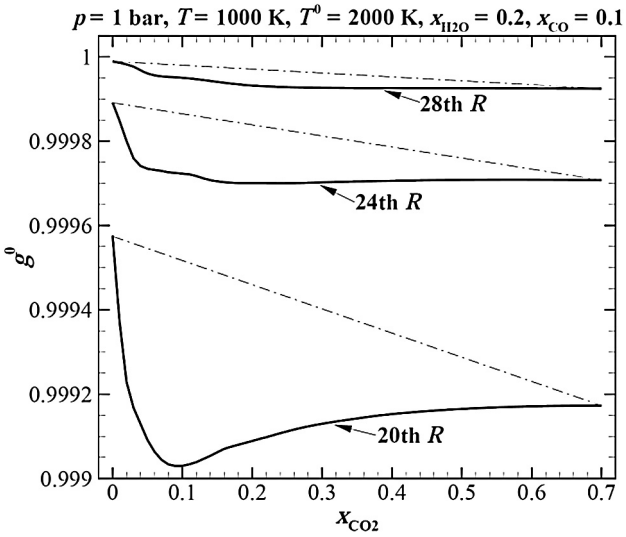

Fig. 3. Exact g^0-values corresponding to 20th, 24th and 28th fixed R-values with increasing mole fraction of CO_2 using a 32-point Gauss-Chebyshev quadrature scheme. (dash-dot lines represent linear lines connecting the first and the last exact values).

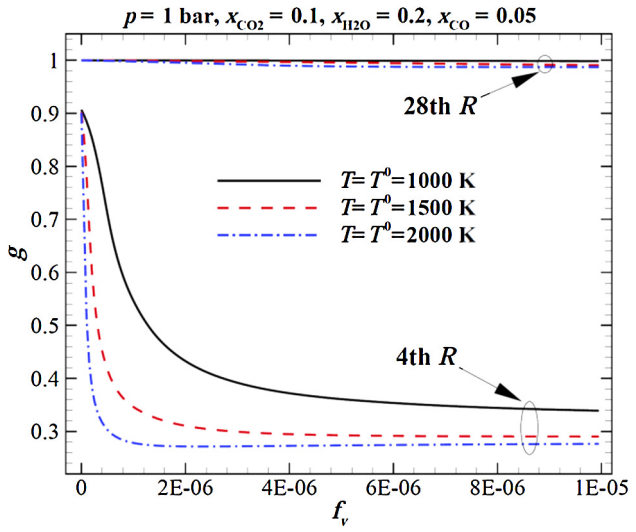

Fig. 4. Exact g^0-values corresponding to two fixed R-values with increasing volume fraction of soot at three temperatures using a 32-point Gauss-Chebyshev quadrature scheme.

an exponentially decreasing trend as seen in Fig. 4. Therefore, additional soot volume fraction data points are also required to decrease nonlinear effects, especially at low soot volume fractions. In the current random-number database, the required gas mole fractions and soot volume fractions to guarantee high accuracy using 7-D linear interpolation for most radiative calculations are listed in Table 1, in which pressures, local temperatures and reference temperatures are also summarized. Compared to the data points in the FSCK look-up table, three additional CO_2 mole fractions (0.1, 0.15 and 0.2) and two additional soot volume fractions (10^{-7} and 10^{-6}) were added to the random-number database in order to mitigate the nonlinear behavior. Since the construction of a random-number database always requires correlated k-values, the same extension has been included in the latest FSCK look-up table.

Since the nonlinearities depend on pressure, gas temperature, reference temperature, concentrations and quadrature points, complete removal of nonlinear effects is impossible. This means data interpolated from the tabulated values in Table 1 may result in some errors. For most cases, the errors due to nonlinearities using the tabulated values in Table 1 are very small, and details are presented in Section 4. However, undiscovered nonlinearities may still exist that can lead to considerable error. Therefore, like the FSCK look-up table, the random-number database is stored separated by pressure, mole fractions of three gases and volume fraction of soot, each of which requires approximate 100 kB for storage. In addition, the memory management approach proposed in [7] is also applied for loading the required data directly from those individual files into memory. This makes it convenient to add additional required files into the databank for the sake of mitigating nonlinear effects if undiscovered nonlinearities are found in the future.

As mentioned in Section 2.1, the SLW (or ADF) method is mathematically identical to the FSCK method, although SLW and ADF traditionally use less accurate stepwise integration. The random-number database developed in this work is also valid for these methods, and values of $\tilde{k}_i(T_P, \boldsymbol{\phi})$ and $\bar{a}_i(T_P, T^0)$ can be readily obtained from the FSCK look-up table, just replacing $k^*(g_i^0)$ and $a(g_i^0)$ by $\tilde{k}_i(T_P, \boldsymbol{\phi})$ and $\bar{a}_i(T_P, T^0)$, respectively, to combine them with a PMC solver. Very recently, it has been shown that SLW can be used with Gaussian integration [32], for which the required gray gas absorption coefficients and their weights can also be obtained from the present look-up table.

4. Flame calculations

To test the accuracy of the random-number database, radiative heat transfer for two scaled flames is calculated using the PMC solver combined with the FSCK method. The first flame named Sandia D × 4 by [33] is a nonluminous flame without soot, while the other one named Flame VII by [34] is a luminous flame with soot. Both flames are simulated with a two-dimensional axisymmetric mesh, and only quasi-steady time-average profiles are used for radiative calculation comparisons, i.e., TRI is not considered. The negative radiative heat source, $\nabla \cdot q$, is determined using the PMC solver combined with both LBL or FSCK method without feedback to the flame and the volumetric emission is given by the optically thin (OT) solver. The benchmark LBL calculations here still employ the random-number database for the LBL/PMC method as developed in [21]. For the FSCK/PMC method, the radiative properties obtained from the FSCK look-up table are determined by the g^0-R relation in the random-number database developed in this work. In all PMC calculations, 10 runs/trials are carried out with 1,000,000 photon rays used for each test to make the standard deviations as small as possible.

Figs. 5 and 6 show the distributions of both volumetric emission and $\nabla \cdot q$ at two axial locations for Sandia D × 4 and Flame VII, respectively. The standard deviations for $\nabla \cdot q$ are shown as error bars and are very small, demonstrating the high confidence of

Table 1
Precalculated thermodynamic states in random-number database.

Parameters	Range	Values	Number of points
Species	CO_2, H_2O, CO and soot	–	–
Pressure (total)	0.1–0.5 bar	Every 0.1 bar	34
	0.7 bar	0.7 bar	
	1.0–14.0 bar	Every 1.0 bar	
	15.0–80 bar	Every 5 bar	
Local temperature	300–3000 K	Every 100 K	28
Reference temperature	300–3000 K	Every 100 K	28
Mole fraction of CO_2	0.0–0.05	Every 0.01	13
	0.1–0.2	Every 0.05	
	0.25–1.0	Every 0.25	
Mole fraction of H_2O	0.0–0.05	Every 0.01	13
	0.1–0.2	Every 0.05	
	0.25–1.0	Every 0.25	
Mole fraction of CO	0.0–0.5	[0.0, 0.01, 0.05, 0.1, 0.25, 0.5]	6
Volume fraction of soot	0.0–10^{-5}	[0.0, 10^{-7}, 10^{-6}, 10^{-5}]	4

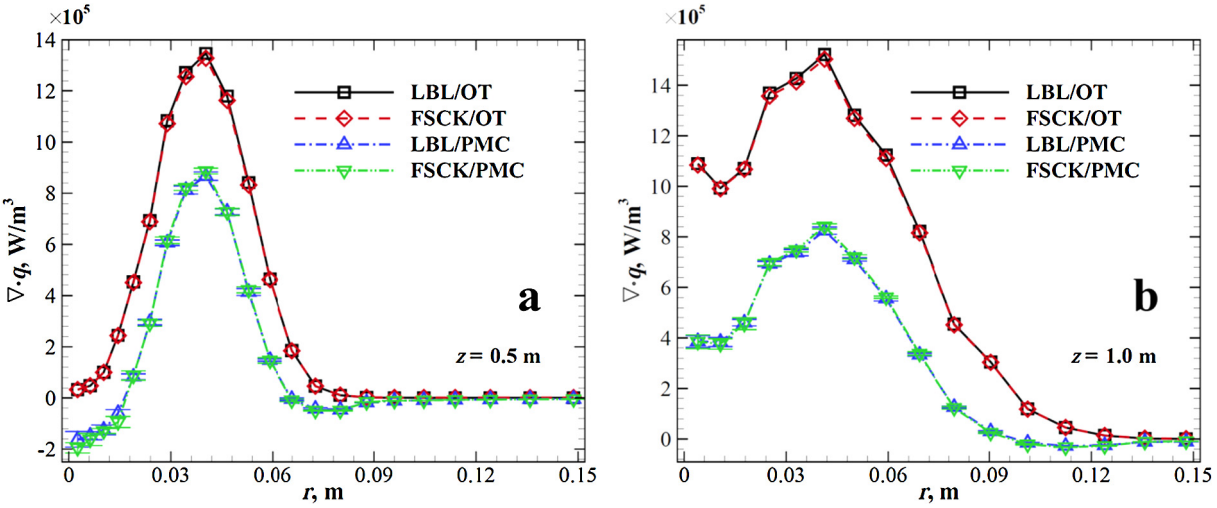

Fig. 5. Comparison of negative radiative heat source for Sandia D × 4 using different methods at two locations, (a) $z = 0.5$ m, (b) $z = 1.0$ m.

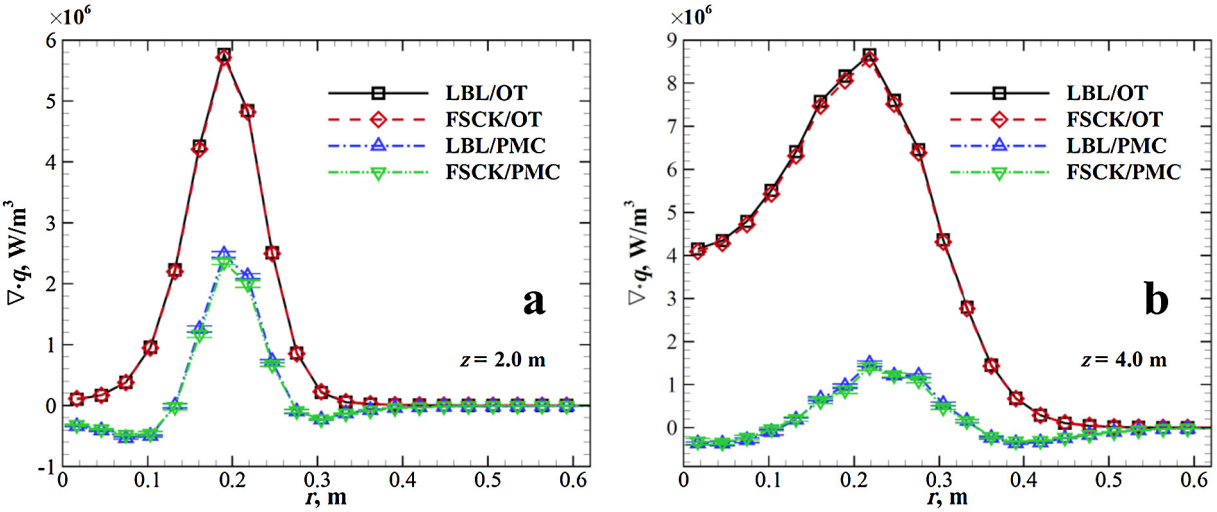

Fig. 6. Comparison of negative radiative heat source for Flame VII using different methods at two locations, (a) $z = 2$ m, (b) $z = 4$ m.

Table 2
Comparison of average CPU time and memory requirement per run for PMC solvers combined with different spectral methods; 10 runs.

Method	Sandia D4 CPU time (s)		Flame VII	
	Spectral variable selection	Ray tracing	Spectral variable selection	Ray tracing
LBL/PMC	0.05	111.54	0.11	145.55
FSCK/PMC	0.02	84.76	0.11	121.12
	Memory requirement (MB)			
LBL/PMC	1126.4		1228.8	
FSCK/PMC	53.5		148.3	

the calculations. Results using the FSCK look-up table have been presented in [7], which demonstrated that the FSCK look-up table exhibits excellent accuracy compared with the benchmark LBL calculations. Therefore, volumetric emission, as expected, is well predicted when using the FSCK/OT method for both flames. The negative radiative heat source, $\nabla \cdot q$, calculated by the FSCK/PMC method for the two flames at both locations, shows good agreement with those using the LBL/PMC method. Some errors due to nonlinearities from both the FSCK look-up table and the random-number database can be found in the figures. However, the differences appear to be relatively small, illustrating that the random-number database can be accurately applied to both gaseous media and gas-soot mixtures.

For the PMC simulations, the average CPU cost per run can be divided into two parts as shown in Table 2, i.e., spectral variable selection and ray tracing. Spectral variable selection means assigning a wavenumber η (in the LBL/PMC method) or an artificial wavenumber g^0 (in the FSCK/PMC method) to photon rays during initialization, while during ray tracing evaluation of one spectral property is required for each cell traversed. From Table 2, it is found that ray tracing consumes most of the CPU time in the PMC calculations. For the LBL/PMC method, to find one spectral property

one must first calculate two surrounding values by interpolations from the databased LBL absorption coefficients, followed by interpolation of spectral properties from the surrounding values to find the desired cell variable. This requires pre-loading the huge number of spectral LBL absorption coefficients at each thermodynamic state into memory. As seen from Table 2, LBL/PMC calculations for both flames require more than 1000 MB memory, most of which are used for storing a half million databased values at 1 bar for each gas component. Memory requirement for Flame VII is slightly larger than that for Sandia D × 4 because of a finer mesh (10,000 for Flame VII and 3325 for Sandia D × 4). Due to the huge memory requirement for LBL/PMC databases, the surrounding values must be calculated on-the-fly during ray tracing, or it may result in unacceptable memory cost, and thus increases CPU time significantly.

In contrast, for the FSCK/PMC method there are only 33 k-values (32 correlated k-values corresponding to g^0-quadratures plus one maximum k-value) at each thermodynamic state, so that the correlated k-distributions for each cell can be calculated and loaded into the memory during the initialization of the FSCK/PMC method without affecting efficiency or requiring much memory. This is well illustrated in Table 2, where both the average CPU cost of spectral variable selection (which includes the calculations of correlated k-distributions for each cell) and the memory requirement for the FSCK/PMC method is very low. More importantly, during ray tracing for the FSCK/PMC method, calculations of surrounding values can be eliminated and spectral properties can be directly obtained from the pre-loaded k-distributions of each cell. As a result, with the FSCK/PMC method CPU time is reduced considerably during ray tracing as shown in Table 2. Together with the accuracy consideration mentioned above, the FSCK/PMC method using the FSCK look-up table and the random-number database developed in this work provides an excellent alternative for radiative calculations. Moreover, the FSCK/PMC method also provides a benchmark solution to test the accuracy of conventional RTE solvers combined with the FSK/FSCK method in multi-dimensional geometries.

5. Conclusions

In this work, the FSCK look-up table developed by the authors has been successfully combined with a PMC solver by developing a random-number database storing g^0-R relations for use with the FSCK/PMC method. Similar to the FSCK look-up table, the random-number database includes CO_2, H_2O, CO and soot, and has the same range of thermodynamic states, i.e., pressure ranges from 0 to 80 bar, temperature ranges from 0 to 3000 K, mole fractions of CO_2 and H_2O range from 0 to 1 while that of CO ranges from 0 to 0.5 and the volume fraction of soot ranges from 0 to 10^{-5}.

Radiation modeling for two realistic, scaled flames was carried out to test the performance of the random-number database. The results indicate that compared to benchmark LBL calculations, almost the same accuracy can be achieved using the FSCK/PMC method with FSCK look-up table and random-number database, while the ray tracing process becomes roughly 20% more efficient and memory requirement is greatly reduced. Therefore, there are two important applications for the FSCK/PMC method: (1) Applications where the savings in memory and CPU time vs. LBL/PMC are important, and (2) as a benchmark to test the accuracy of conventional RTE solvers paired with the FSCK spectral model.

The random-number database is available from the corresponding author's website upon request at http://eng.ucmerced.edu/people/mmodest.

Conflicts of interest

The authors declare that there are no known conflicts of interest.

Acknowledgments

This work was financially supported by "the Fundamental Research Funds for the Central Universities", Grant No. 2018JBM047, and "the National Natural Science Foundation of China", Grant No. 51576014.

References

[1] M.F. Modest, The treatment of nongray properties in radiative heat transfer: From past to present, ASME J. Heat Transf. 135 (2013) 061801-1–061801-12.
[2] J.O. Arnold, E.E. Whiting, G.C. Lyle, Line-by-line calculation of spectra from diatomic molecules and atoms assuming a voigt line profile, J. Quant. Spectrosc. Radiat. Transf. 9 (6) (1969) 775–798.
[3] M.F. Modest, Narrow-band and full-spectrum k-distributions for radiative heat transfer-correlated-k vs. scaling approximation, J. Quant. Spectrosc. Radiat. Transf. 76 (1) (2003) 69–83.
[4] C.J. Wang, W.J. Ge, M.F. Modest, B.S. He, A full-spectrum k-distribution look-up table for radiative transfer in nonhomogeneous gaseous media, J. Quant. Spectrosc. Radiat. Transf. 168 (2016) 46–56.
[5] C.J. Wang, M.F. Modest, B.S. He, Full-spectrum k-distribution look-up table for nonhomogeneous gas-soot mixtures, J. Quant. Spectrosc. Radiat. Transf. 176 (2016) 129–136.
[6] C.J. Wang, M.F. Modest, B.S. He, Improvement of full-spectrum k-distribution method using quadrature transformation, Int. J. Therm. Sci. 108 (2016) 100–107.
[7] C.J. Wang, M.F. Modest, B.S. He, Efficient full-spectrum correlated-k-distribution look-up table, J. Quant. Spectrosc. Radiat. Transf. 219 (2018) 108–116.
[8] W.J. Ge, R. Marquez, M.F. Modest, S.P. Roy, Implementation of high-order spherical harmonics methods for radiative heat transfer on OpenFOAM, ASME J. Heat Transf. 137 (2015) 052701-1–052701-9.
[9] W.J. Ge, M.F. Modest, R. Marquez, Two-dimensional axisymmetric formulation of high order spherical harmonics methods for radiative heat transfer, J. Quant. Spectrosc. Radiat. Transf. 156 (2016) 58–66.
[10] P.J. Coelho, Advances in the discrete ordinates and finite volume methods for the solution of radiative heat transfer problems in participating media, J. Quant. Spectrosc. Radiat. Transf. 145 (2014) 121–146.
[11] J. Cai, S.P. Roy, M.F. Modest, A comparison of specularly reflective boundary conditions and rotationally invariant formulations for Discrete Ordinate Methods in axisymmetric geometries, J. Quant. Spectrosc. Radiat. Transf. 182 (2016) 75–86.
[12] M.F. Modest, Radiative heat transfer, third ed., Academic Press, New York, 2013.
[13] J.R. Howell, M. Perlmutter, Monte Carlo solution of thermal transfer through radiant media between gray walls, ASME J. Heat Transf. 86 (1) (1964) 116–122.
[14] M.F. Modest, The Monte Carlo method applied to gases with spectral line structure, Numer. Heat Transf. Part B-Fundam. 22 (3) (1992) 273–284.
[15] M. Cherkaoui, J.L. Dufresne, R. Fournier, J.Y. Grandpeix, A. Lahellec, Monte Carlo simulation of radiation in gases with a narrow-band model and a net-exchange formulation, ASME J. Heat Transf. 118 (2) (1996) 401–407.
[16] J.T. Farmer, J.R. Howell, Monte Carlo prediction of radiative heat transfer in inhomogeneous, anisotropic, nongray media, J. Thermophys. Heat Transf. 8 (1) (1994) 133–139.
[17] J.T. Farmer, J.R. Howell, Comparison of Monte Carlo strategies for radiative transfer in participating media, in: J.P. Hartnett, T.F. Irvine (Eds.), Advances in Heat Transfer, vol. 31, Academic Press, New York, 1998.
[18] A.Q. Wang, M.F. Modest, Spectral Monte Carlo models for nongray radiation analyses in inhomogeneous participating media, Int. J. Heat Mass Transf. 50 (2007) 3877–3889.
[19] T. Ozawa, M.F. Modest, D.A. Levin, Spectral module for photon Monte Carlo calculations in hypersonic nonequilibrium radiation, ASME, J. Heat Transf. 132 (2) (2010), pp. 023406–023406-8.
[20] A. Feldick, M.F. Modest, An improved wavelength selection scheme for Monte Carlo solvers applied to hypersonic plasmas, J. Quant. Spectrosc. Radiat. Transf. 112 (2011) 1394–1401.
[21] T. Ren, M.F. Modest, A hybrid wavenumber selection scheme for line-by-line photon Monte Carlo simulations in high-temperature gases, ASME J. Heat Transf. 135 (2013), 084501–084501 4.
[22] L. Wang, J. Yang, M.F. Modest, D.C. Haworth, Application of the full-spectrum k-distribution method to photon Monte Carlo solvers, J. Quant. Spectrosc. Radiat. Transf. 104 (2007) 297–304.
[23] M.K. Denison, B.W. Webb, A spectral line-based weighted-sum-of-gray-gases model for arbitrary RTE solvers, ASME J. Heat Transf. 115 (4) (1993) 1004–1012.
[24] F. Liu, H. Chu, H. Zhou, G.J. Smallwood, Evaluation of the absorption line blackbody distribution function of CO_2 and H_2O using the proper orthogonal decomposition and hyperbolic correlations, J. Quant. Spectrosc. Radiat. Transf. 128 (2013) 27–33.
[25] J.T. Pearson, B.W. Webb, V.P. Solovjov, J. Ma, Effect of total pressure on the absorption line blackbody distribution function and radiative transfer in H_2O, CO_2, and CO, J. Quant. Spectrosc. Radiat. Transf. 143 (2014) 100–110.

[26] J.T. Pearson, B.W. Webb, V.P. Solovjov, J. Ma, Efficient representation of the absorption line blackbody distribution function for H_2O, CO_2, and CO at variable temperature, mole fraction, and total Pressure, J. Quant. Spectrosc. Radiat. Transf. 138 (2014) 82–96.
[27] G. Węcel, Z. Ostrowski, P. Kozołub, Absorption line black body distribution function evaluated with proper orthogonal decomposition for mixture of CO_2 and H_2O, Int. J. Numer. Meth. Heat Fluid Flow 24 (4) (2014) 932–948.
[28] M.F. Modest, V. Singh, Engineering correlations for full spectrum *k*-distribution of H_2O from the HITEMP spectroscopic databank, J. Quant. Spectrosc. Radiat. Transf. 93 (2005) 263–271.
[29] A.Q. Wang, Investigation of turbulence-radiation interaction in turbulent flames using a hybrid finite volume/Monte Carlo approach PhD thesis, Pennsylvania State University, Pennsylvania, 2007.
[30] L.S. Rothman, I.E. Gordon, R.J. Barber, H. Dothe, R.R. Gamache, A. Goldman, et al., HITEMP, the high-temperature molecular spectroscopic database, J. Quant. Spectrosc. Radiat. Transf. 111 (15) (2010) 2139–2150.
[31] H. Chang, T.T. Charalampopoulos, Determination of the wavelength dependence of refractive indices of flame soot, in: Proceedings of the Royal Society, London, 1990, pp. 577–591.
[32] V.P. Solovjov, F. Andre, D. Lemonnier, B.W. Webb, The rank correlated SLW model of gas radiation in non-uniform media, J. Quant. Spectrosc. Radiat. Transf. 197 (2017) 26–44.
[33] G. Pal, A. Gupta, M.F. Modest, D.C. Haworth, Comparison of accuracy and computational expense of radiation models in simulation of non-premixed turbulent jet flames, Combust. Flame 162 (6) (2015) 2487–2495.
[34] R.S. Mehta, M.F. Modest, D.C. Haworth, Radiation characteristics and turbulence-radiation interactions in sooting turbulent jet flames, Combust. Theor. Model. 14 (1) (2010) 105–124.